Title
A neurobiological theory of meaning in perception. Part 5. Multicortical patterns of phase modulation in gamma EEG

Journal
International Journal of Bifurcation & Chaos, 13

Authors
Freeman, Walter J, III
Rogers, Linda J

Publication Date
2003

Peer reviewed

A neurobiological theory of meaning in perception.

Part 5. Multicortical patterns of phase modulation in gamma EEG

International Journal of Bifurcation & Chaos [2003] 13: 2867-2887.

Walter J Freeman
Linda J Rogers

Department of Molecular & Cell Biology
University of California
Berkeley CA 94720-3200 USA
dfreeman@berkeley.edu
drljrogers@home.com

Key words: analytic phase, beta oscillation, EEG synchronization, gamma oscillation, Hilbert transform, phase transition

Running Title: Global episodic beta/gamma synchrony

ABSTRACT

The aim of this study was to find evidence for repetitive global phase transitions occurring simultaneously over multiple areas of cortex during normal behavior. EEGs were recorded from multiple high-density arrays of 14-16 electrodes surgically fixed on the visual, auditory, somatomotor, and entorhinal cortices of trained cats and rabbits, and from a linear array of 64 electrodes on the scalp of volunteers. Analytic phase relations between gamma EEG signals from multiple cortices were examined with high temporal resolution provided by the Hilbert transform. An index of synchronization was applied to intercortical pairs of signals to detect and display epochs of engagement between pairs. The measure was adapted to derive an index of global synchronization among all 4 cortices that was calculated as a t-value. Global epochs of phase stabilization ('locking') were found to involve all cortices under observation. The phase values were not clustered at zero but were in distributions about nonzero means. Episodic destabilization (decoherence) occurred aperiodically at intervals corresponding to rates in the delta range, with equal likelihood before the onset of the conditioned stimuli (CSs) and in post-stimulus test periods including performance of conditioned responses (CRs). Preferential pairwise phase stabilization was sought but not found between the sensory cortex receiving the auditory or visual CSs and the entorhinal or somatomotor cortex at times of CSs or CRs. The cospectrum from cross-correlating the global synchronization index with the global spatial ensemble average of the unfiltered EEG peaked in the delta range (1-3 Hz) near 2.5 Hz in cat and below 2 Hz in rabbit. The cospectrum of the EEG with the derivative of the analytic phase in humans peaked in the alpha range (7-12 Hz) The results indicated that macroscopic states of synchronized neural activity related to Gestalts formed during perception, that included the primary sensory and limbic areas and perhaps the entire neocortex of each cerebral hemisphere.

1. INTRODUCTION

The search for neural correlates of discriminative conditioned stimuli (CSs) in the EEGs of sensory cortices has led to several dead ends and surprising turns [Freeman, 2003a]. The first hypothesis for spatial coding in olfaction was Adrian's [1950], predicting that neural responses to differing odorants would be localized in different areas of the bulb. A test of this hypothesis with multielectrode EEGs failed to confirm localization of responses [Freeman & Schneider, 1978], but it led to a new hypothesis, that the bulb maintained a search image for an expected CS [Freeman, 1983]. The representation of a sought-for odor was conceived to have the form of a spatial pattern of amplitude modulation (AM) of bulbar gamma oscillation [Freeman, 1979]. Arrival of an anticipated stimulus would be signaled by a collapse of the already documented broad pre-stimulus phase distribution, leading to enhanced bulbar output [Freeman, 1980]. Improved measurement of EEG phase and amplitude [Freeman & Viana Di Prisco, 1986] disproved this hypothesis in two respects. The AM patterns were not invariant with respect to the CSs [Freeman & Grajski, 1987], and there was no collapse of the phase distribution on CS arrival [Freeman & Baird, 1987].

A new hypothesis was proposed, that the bulb maintained an attractor landscape, which was activated by sensory input under limbic control through a phase transition. When the landscape was brought into play, the stimulus selected one of the basins [Skarda & Freeman, 1987]. When the bulb was confined by convergence to the attractor, the neurodynamics constructed and transmitted an AM pattern that was correlated with the meaning of the CS for the subject. This hypothesis was successfully tested in the bulb by serial conditioning [Freeman & Davis, 1990; Freeman, 1991] and discriminative learning with contingency reversal [Freeman & Grajski, 1987]. The model was successfully extended to the visual, auditory and somatomotor cortices [Barrie, Freeman & Lenhart, 1996]. The hypothesis of AM pattern formation by phase transition was supported by measuring the phase gradients of the gamma oscillations of wave packets [Freeman & Barrie, 2000; Freeman, 2003b]. Calculating the analytic phase with the Hilbert transform [Freeman & Rogers, 2002]showed that the numerical derivative of the phase had spikes at the recurrence rates of the AM patterns and the stable spatial patterns of phase modulation (PM) in neocortical EEGs.

The search for multisensory correlates of CSs in EEGs manifesting Gestalts has also taken a winding path. The first hypothesis was that a wave packet would be found in the primary sensory area to which the CS was directed. The content would have the form of a spatial AM pattern on a carrier wave in the gamma frequency range. The packet would be transmitted to other cortices, especially the entorhinal and somatomotor cortices, by a brief episode of phase locking between the transmitting and receiving cortices. A phase lag would be found by time-lagged correlation that would correspond to the conduction delay between them. The amplitude of activity in the receiving cortex would show a transient burst, owing to resonance with the oscillatory wave packet coming from the transmitting cortex. No evidence was found for these characteristics [Freeman, Gaál & Jornten, 2003]. Instead, the maximal time-lagged correlation was always at zero delay, and a sustained covariance was found among all areas. As measured by PCA, half the power was coherent in the gamma band after spatial ensemble averaging.

A new hypothesis was put forth, that intermittent AM patterns would be found involving all areas. This model was based on the premise that, just as neurons forming a wave packet retain a high degree of autonomy while participating in the whole, widely separated areas of cortex likewise would function quasi-independently while cooperating in the formation of a large-scale pattern of activity. The test was to calculate in a moving window the root mean square (RMS) amplitudes of all available EEGs in the several recording sites, express them as points in 64-space, search for clusters corresponding to the three CSs (none, CS0, with reinforcement, CS+, and without, CS-), and measure the probability of correct classification using the Euclidean distance of points from test trials to centers of gravity determined on training trials, just as was done in finding AM patterns in wave packets.

The results [Freeman & Burke, 2003] supported the hypothesis by showing classification of AM patterns with respect to CSs well above chance levels. The most important aspect was the decrease in goodness of classification caused by removal of the signals from any of the five areas included. The results depended on pooling across subjects and sessions, and they failed to show evidence of the local wave packets that were predicted to occur in the sensory areas to which the CSs were directed. The reason proposed for these weaknesses in the evidence was the small number of electrodes available. Obviously the experiment should be repeated with 128 to 256 electrodes. Yet the data on hand permitted testing a new corollary hypothesis, that the spatial patterns of phase in the gamma range would reveal global episodes of stabilization in fixed, non-zero distributions lasting on the order of a tenth of a second. As with wave packets, the stable PM patterns would be interrupted by episodic decoherence, with peaks in the phase derivative recurring in the theta (3-7 Hz) and upper delta (1-3 Hz) ranges of the EEG. The phase locking and destabilization would involve all areas. The test of this hypothesis using the Hilbert transform was the aim of this report. As a supplement to the cat and rabbit data, testing was also done on EEGs recorded from the scalp of human volunteers in a state of relaxed awareness, in search of global phase stabilization in the gamma range with episodic decoherence. Again the results gave surprising, on this occasion in species differences, because the phase stabilization was optimally in the beta range (12-20 Hz) and not the gamma range, and the recurrence rates were preferentially in the alpha range (7-12 Hz) rather than the lower theta and upper delta ranges found in cats and rabbits.

2. METHODS

2.1. Animal studies

Methods for preparation of animal subjects, data collection, and data processing have been described in detail in prior reports [Barrie, Freeman and Lenhart, 1996; Gaál and Freeman, 1998; Freeman and Rogers, 2002; Freeman, Gaál & Jornten, 2003]. The Hilbert transform was by the Cauchy integral to extract the Principal Value, equivalent to taking the local derivative at each time point in each trace and generating a complex number. The analytic amplitude, v(t), was given by the square root of the sum of squares of the two parts, and the analytic phase, $\phi(t)$, was given by the arc-tangent [Barlow 1993; Hahn 1996; Stearns and David 1996]. Branching of the arc-tangent occurred whenever the phase approached $\pm\pi/2$, giving a sawtooth function. A continuously increasing function of time was given by unwrapping the arc-tangent function. The procedure in Matlab [Stearns and David 1996] used a constant threshold for detecting phase jumps near $\pm\pi/2$. Its results were inconsistent. It missed some breaks that needed unwrapping, because the phase jumps were not of the same size, and it falsely detected phase jumps that occurred, when the EEG did not cross zero. An empirical procedure that worked well was to detect zero-crossings directly in the EEG and unwrap at those locations [Freeman & Rogers, 2002]. The atan2(im,real) was also tested but gave less reliable results. The Hilbert transform required band pass filtering when applied to aperiodic signals with $1/f^{\alpha}$ spectra like EEGs [Quiroga et al., 2002]. Otherwise the analytic phase resembled a random walk. In this study the pass band for optimal AM pattern classification was used to define the gamma range, which differed between rabbits, 20-80 Hz [Barrie, Freeman and Lenhart 1996] and cats, 35-60 Hz [Gaál and Freeman 1998].

Studies of the distributions of phase values and phase differences between channels was facilitated by recognition of the stabilization of spatial phase differences in EEGs for varying time windows {Freeman & Barrie, 2000; Freeman & Rogers, 2002; Freeman, 2003b], leading to partitioning of the variance into temporal and spatial components, where $\phi_x(t)$ was defined as the analytic phase for channel x as function of time.

$$\Phi_x(t) = 1/2n \sum_{\tau = t-n}^{\tau = t+n} \phi_x(\tau), \quad x = 1, N, \tag{1}$$

where N = number of channels, 14-16, and 2n = window size = 40 samples at 2 ms intervals. The normalized phase difference for each pair was given by

$$\Delta\phi_{x2,1}(\tau) = [\phi_{x2}(\tau) - \Phi_{x2}(t)] - [\phi_{x1}(\tau) - \Phi_{x1}(t)] \tag{2}$$

The spatial standard deviation was given by

$$SD_x(t) = \{ 1/np \, [\sum_{x1=1}^{N-1} \sum_{x2=x1+1}^{N} 1/(2w-1) \sum_{\tau = t-n}^{\tau = t+n} [\phi_{x1}(\tau) - \Phi_{x1}(t) - (\phi_{x2}(\tau) - \Phi_{x2}(t))]^2]\}^{.5} \tag{3}$$

where np = all possible pairs of channels. The temporal standard deviation was given by

$$SD_t(t) = \{\ 1/N \sum_{x=1}^{N} 1/(2n-1) \sum_{\tau=t-n}^{\tau=t+n} [\phi_x(\tau) - \Phi_x(t)\ ]^2\ \}^{.5}. \qquad (4)$$

The time series, $SD_x(t)$ and $SD_t(t)$, were obtained by repeating the calculations while stepping the window in 10 msec intervals. They were generalized to a global measure for a group of channels by the root mean square. The utility of this measure lay in its independence from the mean of the phase differences maintained between all channel pairs, which varied across the groups (up to 16 electrodes in 4x4 mm windows on 4 cortices in 4 cats and 3 rabbits). $SD_x(t)$ varied inversely with synchronization and was used as a decoherence index. The values of $\Delta\phi_{\tau,\xi}(t)$, $SD_t(t)$, or $SD_x(t)$ were pooled in histograms to determine their distributions, as the basis for devising levels of significance for indices of the phase variation coarse-grained by the 80 msec window.

A pairwise index of synchronization was adapted from a method developed by Pikovsky, Rosenblum & Kurths [2001] and used Tass et al. [1999] to define statistical phase locking as a peak in the distribution of the phase differences between pairs of traces within a sliding window, based on normalized Shannon entropy:

$$e(t) = = \sum_{j=1}^{N} p_j \ln p_j\ , \qquad (5)$$

where p_j was the relative frequency of finding the phase mod 2π within the j-th bin, and e varied between zero and $\hat{e} = \ln N$, the number of bins (e.g. 100 bins of 0.06 radians between $-\pi$ and $+\pi$ radians). This synchronization index as a function of time was normalized,

$$q(t) = (\ \hat{e}-e(t))/\hat{e}, \qquad (6)$$

so that q(t) was zero for a uniform distribution, and one for a delta distribution of phase values. Significance was inferred by comparing the values derived from the experimental data with results from white noise (time series of normally distributed random numbers with zero mean and unit standard deviation, filtered, truncated to 12 bits, and otherwise treated in the same way as the EEG data). Another control was the use of 'shuffled' time series, in which the start of each window was randomly re-set independently on each channel, and the beginning segment was transposed and re-attached to the end. Each channel's phase time series of n points in a time window, $\phi_\xi(t)$, was replaced by $\phi_y(t)$, where

$$\phi_y(t) = (\phi_\xi(k, k+1,...,n), \phi_\xi(1, 2,...,k-1)), \qquad (7)$$

and k was a point chosen from a uniformly distributed random variable with values from 1 to n. This shuffling in time guaranteed the independence of the phase series in the traces.

The synchronization index, q(t), was generalized to multiple channels by calculating the distribution of phase differences over all pairs of channels, after subtracting the means for each pair within the 80 msec sliding window as in equation (3). This procedure imposed near-zero mean on all pairs, in order to document the phase locking of multiple traces that were fluctuating together in the gamma range but with phase differences that were transiently fixed at different

values for every pair of traces, as found in the phase gradients in all primary sensory receiving areas.

An intercortical index was devised from pairs of cortices by using all pairs of channels from the two cortices (excluding those pairs within one cortex). An average of the 6 values of q(t) from 4 pairs of cortices, Q(t), was calculated for both cat and rabbit data sets, for which four arrays of 14-16 electrodes had been fixed on 4x4 mm areas of differing cortices. The distributions of Q were nearly Gaussian, and they were derived from 4 independent measures at successive time points. On this basis a global intercortical macroscopic synchronization index was derived from Q as a t-value, t_Q (d.f. = 3 for a one-tailed test of the mean > 0 over 4 cortices). This index was given by the mean of Q from the 6 pairs among the 4 cortices in each window, divided by the standard error of the 6 values in the window. Values of t_Q in successive windows were plotted as a time series. A shuffled intercortical control was calculated as y(t) = [x(k, k+1,...,m), x(1, 2,...,k-1)], where x(t) was the original phase time series of m points for one channel, and k was a point chosen from a uniformly distributed random variable with values from 1 to m. Autocorrelations and crosscorrelations were calculated for $t_Q(t)$ and both local and the global spatial ensemble averages of unfiltered EEG, followed by the autospectra and cospectra for cat and rabbit data.

2.2. Human studies

Adult volunteers were asked to sit quietly and relax with eyes closed and then with eyes open. The data were collected in the EEG Clinic of Harborview Hospital, University of Washington, Seattle, and sent by ftp without identifying markers of personal information to the University of California at Berkeley. Data collection was governed by protocols approved by the Helsinki Declaration and the Institutional Review Boards in both institutions. A curvilinear electrode array with 64 gold-plated needles at 3 mm intervals for a length of 18.9 cm was fixed on the scalp paracentrally along the part line. Recordings were referential to the contralateral mastoid. EEGs were amplified with a Nicolet (BMSI 5000) system having a fixed gain of 1628 and analog filters set at 0.5 Hz high pass and 120 Hz low pass. The ADC gave 12 bits with the least significant bit of 0.9 microvolts and a maximal range 4096 bits. The digitizing rate was 200 samples/sec (5 msec interval), while the analog filter was set at 120 Hz, with the possibility of aliasing between 80-100 Hz. Temporal power spectral densities (PSDt) were calculated with the 1-D FFT for every channel after applying a Hanning window to non-overlapping epochs of 1,200 msec. The 64 PSDt were averaged and transformed for display in log-log coordinates. Temporal filters were FIR estimated using Parks-McClellan algorithm of order 200. The transition band width was 4 Hz.

Adult volunteers were asked to sit quietly and relax with eyes closed and then to induce a moderate level of electromyographic activity (EMG) by tightening their scalp muscles without moving. The data were collected by Mark D. Holmes and Sampsa Vanhatalo in the EEG Clinic of Harborview Hospital, University of Washington, Seattle, and sent by ftp without identifying markers of personal information to the University of California at Berkeley. Data collection was governed by protocols approved by the Helsinki Declaration and the Institutional Review Boards in both institutions.

3. RESULTS

3.1. Animal studies

A necessary condition for phase synchronization was a tendency to maintain a constant phase difference between signals from multiple pairs of electrodes over both time and space. Successive values of the spatial differences in phase between all pairs of channels from differing cortices, $\Delta\phi_X(t)$, were calculated. Examples are shown in Fig. 1 of representative phase differences between the 6 pairs of the auditory, somatic, visual and entorhinal cortices, starting at zero at an arbitrary point 1 sec before stimulus onset. The display is comparable to that in Fig. 3 in Freeman and Rogers [2002], using data from the same trial. The time series of differences diverged but not monotonically, with a tendency to epochs of slow rates of change punctuated by short-lasting high rates of change (decoherence) occurring over multiple pairs not quite simultaneously. Whereas the intracortical differences often had sustained plateaus of phase variation giving a staircase appearance, the intercortical differences showed epochs with shallow slopes or 'drift', which was equivalent to small differences in frequency between cortices. The abrupt episodes of intercortical decoherence were comparable to those of intracortical phase differences.

ΦΙΓΥΡΕ ΛΕΓΕΝΔΣ

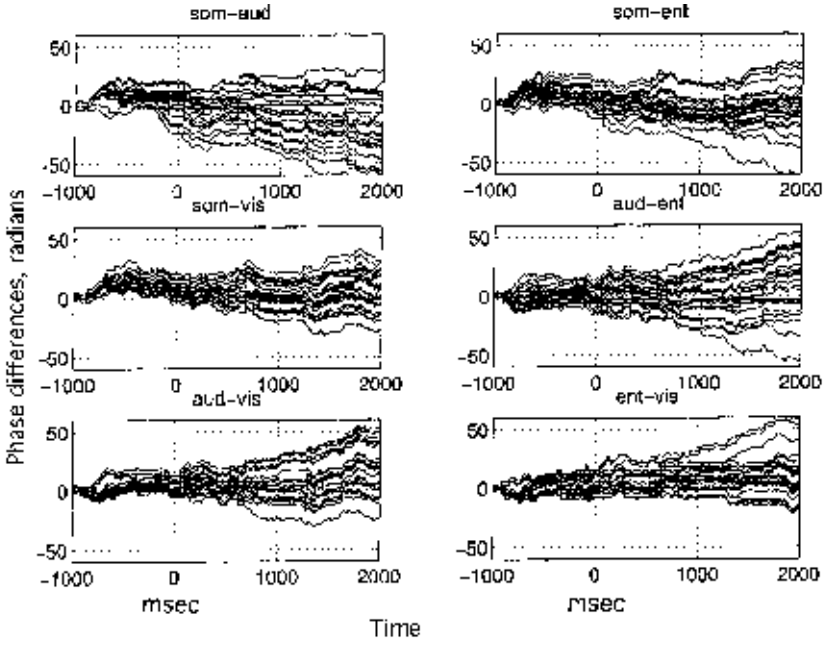

Φιγυρε 1. Τηε ινσταντανεουσ σπατιαλ πηασε διφφερενχεσ, Δφξ, ιν ραδιανσ βετωεεν αν αρβιτραρψ συβσετ οφ 16 χοντιγυουσ χηαννελσ ιν εαχη οφ τηε 4 χορτιχεσ αρε δισπλαψεδ ασ τηεψ εωολωεδ ωιτη τιμε ιν α σινγλε τριαλ ωιτη ΧΣ αρριωαλ ατ 0 μσ.

The intercortical index of synchronization was calculated for intercortical pairs as was previously done for q for intracortical pairs of signals in 80 ms windows stepped every 10 ms. When graphed as time series [Fig. 2, for the same example shown in Fig. 1] the mean synchronization index, q(t) (solid curve), showed sustained levels well above the 99th percentile of the shuffled

control (solid line). For comparison, the intracortical indices for the two cortices, q(t), were also graphed (dashed curves). They were consistently higher than the pairwise intercortical index. The decoherence index [Fig. 2, lower frame] was derived in 80 ms windows by calculating SD_x as a function of time, $SD_x(t)$. The epochs of high synchronization shown by intercortical q(t) were often bracketed by peaks of decoherence that were revealed by high values of SD_x. The intracortical peaks in SD_x were not strictly congruent with each other or with the intercortical peaks, indicating that the underlying state transitions within and between cortices were often dissociated. Systematic exploration of this aspect was deferred pending better understanding of the parameters of intercortical macroscopic states.

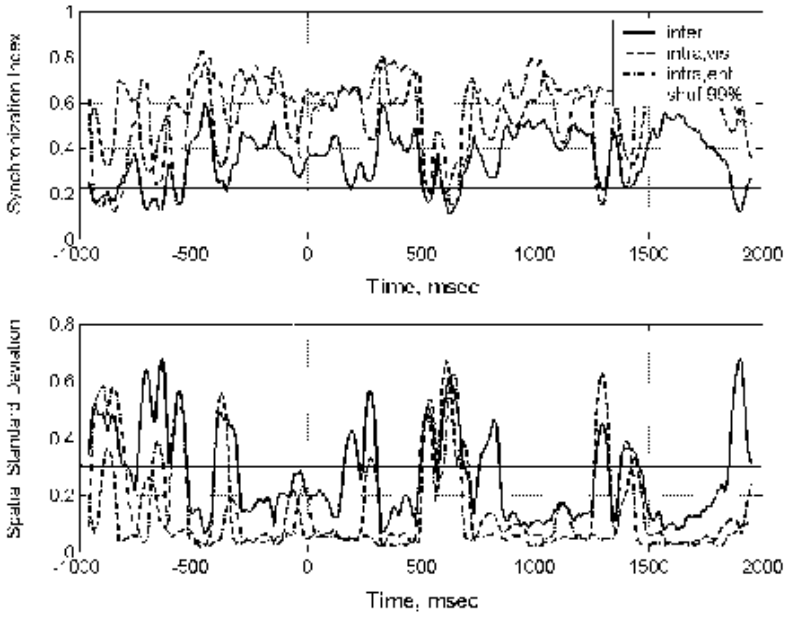

Figure 2. Upper frame: The intercortical index of synchronization, q(t), for intercortical pairs in 80 ms windows stepped every 10 ms was graphed as a time series (solid curve). Values usually lay well above the 99th percentile (0.24) of the shuffled control (solid line) from Figure 3 (upper frame). The intracortical indices, q(t), for the two cortices (dashed curves) occasionally deviated from each other and from the intercortical indices. **Lower frame:** The decoherence index, $SD_x(t)$, showed that the epochs of high synchronization revealed by q(t) were accompanied by periods of low spatial variance in SD_x that were often bracketed by peaks of decoherence shown by high values of SD_x.

Histograms of the intercortical indices [Fig. 3, dark solid curves for the cat data, dark dashed curves for the rabbit data] showed significantly greater synchronization in the gamma EEG compared to the shuffled (dotted curves) and noise (dashed curve) controls. The distributions of Q are shown in the upper frame. For the cat data 62% of the Q synchronization values were above the 99th percentile (0.20) of the noise values (dashed curves), and 48% were above the 99th percentile (0.24) of the shuffled controls (dotted curves). The distributions for SD_x (lower frame) show high values for decoherence and low values for synchronization: 32% of the values of the decoherence index from the cat data were below the 99th percentile (0.31) of the shuffled

control values, and 41% were below the noise 99th percentile (0.35). The distributions of the rabbit data indicated less synchronization, but still were clearly different from the shuffled data and noise controls. With these thresholds the indices were used to test two hypotheses. According to a connectionist view of cortical function, an increase in synchrony should have occurred preferentially between the cortex getting the CS and the entorhinal and/or somatomotor cortices before other areas. According to a holistic view an increase in synchrony should have occurred on average among all areas episodically and preferentially after the CS onset and before the CR onset. Owing to the use of a warning signal at the beginning of each trial with cats but not with rabbits, a possible increase in synchrony was sought prior to CS onset as an indication of an expectancy effect in the cat data but not in the rabbit data.

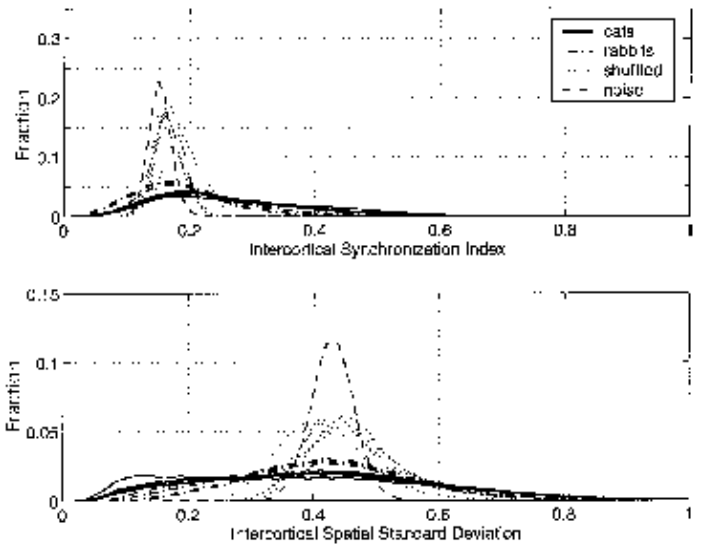

Φιγυρε 3. Υππερ φραμε: Ηιστογραμσ οφ τηε ωαλυεσ οφ τηε ιντερχορτιχαλ σψνχηρονιζατιον ινδεξ, Θ, σηοωεδ γρεατερ σψνχηρονιζατιον ιν τηε γαμμα ΕΕΓ χομπαρεδ το τηε σηυφφλεδ (δοττεδ χυρωεσ) ανδ νοισε (δασηεδ χυρωε) χοντρολσ, γιωινγ τηρεσηολδσ φορ στατιστιχαλ σιγνιφιχανχε: 62% οφ χατ ΕΕΓ ωαλυεσ ωερε αβοωε τηε 99τη περχεντιλε οφ νοισε (0.20) ανδ 48% ωερε αβοωε τηε 99τη περχεντιλε φορ σηυφφλεδ δατα (0.24). **Λοωερ φραμε:** Ιν τηε διστριβυτιονσ οφ τηε δεχοηερενχε ινδεξ, ΣΔξ, τηε σμαλλερ ωαλυεσ ινδιχατεδ σψνχηρονιζατιον: 32% οφ τηε ωαλυεσ φρομ τηε χατ ΕΕΓ ωερε βελοω τηε 99τη περχεντιλε οφ τηε σηυφφλεδ χοντρολ ωαλυεσ (0.31) ανδ 41% ωερε βελοω τηε 99τη περχεντιλε οφ τηε νοισε (0.35).

The results were partially consistent with both hypotheses. The time series, q(t), of the pairwise synchronization index for all six pairs showed frequent peaks above the criterion for significance in both the control and test periods for both cats and rabbits, but not preferentially between the cortex receiving the CS and other areas. An example from a representative trial by a cat [Fig. 4] shows that the pairwise index spiked above the 99th percentile of the intercortical shuffled control (0.24) at rates in the delta range but not in relation to CS onset. Macroscopic synchronization was indicated when the mean, Q, over all six intercortical indices was above the threshold [Fig. 5, upper frame, from a cat).

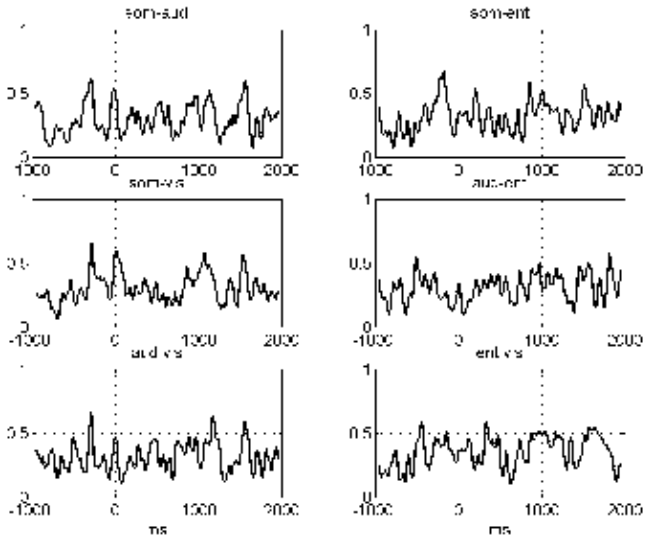

Φιγυρε 4. Αν εξαμπλε οφ τηε τιμε σεριεσ, θ(τ), οφ τηε μεαν οφ παιρωισε σψνχηρονιζατιον ινδεξ ωαλυεσ φορ αλλ σιξ παιρσ φρομ ονε τριαλ σηοωεδ ερρατιχ ινχρεασεσ φορ αλλ παιρσ ωιτη σομε χορρεσπονδενχε βετωεεν τηε παιρσ. Τηερε ωασ νο πρεφερεντιαλ ινχρεασε ιν θ(τ) βετωεεν ανψ παιρ σψστεματιχαλλψ ρελατινγ το ΧΣ ανδ ΧΡ ονσετσ, ασ σηοων βψ ενσεμβλε αωεραγινγ οφ τηεσε σιγναλσ αχροσσ τριαλσ φορ εαχη εξπεριμεντ, ανδ χονφιρμινγ ρεσυλτσ υσινγ τιμε–λαγγεδ χορρελατιον, ΠΧΑ ανδ μυλτιπλε χορρελατιον ον τηεσε δατα [ρεσπεχτιωελψ Φιγυρεσ 8 ανδ 9 ιν Φρεεμαν ετ αλ., 2003].

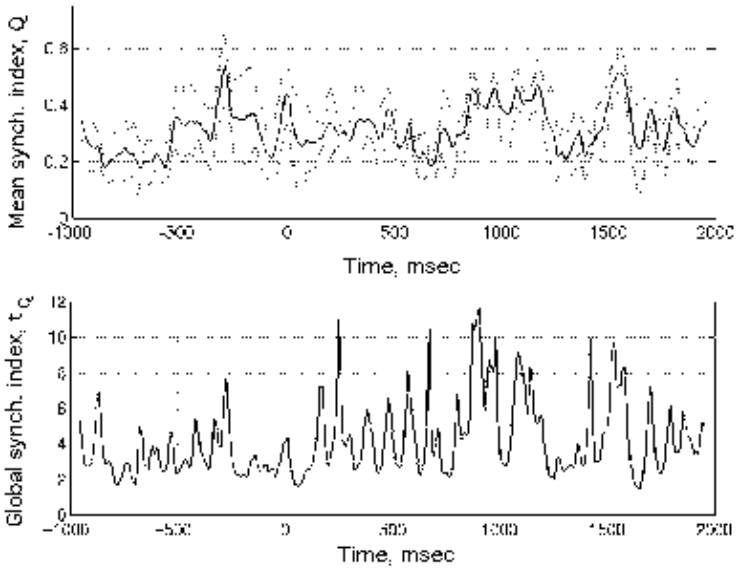

Φιγυρε 5. Υππερ φραμε: Τηε ιντερχορτιχαλ μεαν, Θ(τ), ανδ ιτσ στανδαρδ δεωιατιον αχροσσ τηε 6 παιρσ (νοτ ΣΔξ) αρε σηοων φρομ τηε χυρωεσ οφ θ(τ) ιν Φιγυρε 4. **Λοωερ φραμε:** Τηε ωαλυεσ φορ Θ(τ) ιν τηε υππερ φραμε ωερε χονωερτεδ το τ–ωαλυεσ βψ διωιδινγ τηε μεαν Θ βψ τηε στανδαρδ ερρορ φρομ τηε 6 ωαλυεσ ατ εαχη τιμε ποιντ.

The multiple signals for q(t) were combined in data from both cats and rabbits by plotting the ratio of the global mean, Q, of the 6 values of q at each point in time by the standard error (SE) of the 6 pairs as t-values [Fig. 5, lower frame] giving the macroscopic synchronization index as a function of time, $t_Q(t)$. The locations and time intervals between the peaks in $t_Q(t)$ varied markedly and unpredictably on sequential trials [Fig. 6], so that averaging across trials gave only sustained relatively high levels, corresponding to the high levels of covariance and multiple correlation previously found by linear analyses of these data [Figs. 8 and 9 in Freeman, Gaál & Jornten, 2003]. The t_Q values of the peaks above 4.54 were statistically significant at $p<.01$ by a standard t-test for d.f. = 3 as a convenient threshold. The durations of peaks above that level varied markedly [Fig. 7] with <20% above 76 ms, as previously found for the durations of phase cones in the rabbit data [Freeman, 2002].

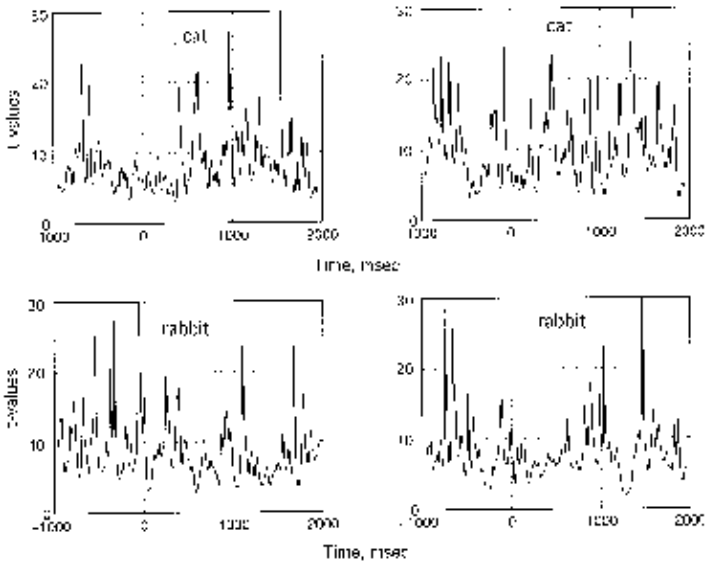

Φιγυρε 6. Φυρτηερ εξαμπλεσ σηοω τηε μαχροσχοπιχ σψνχηρονιζατιον ινδεξ, $\tau_\Theta(\tau)$, γιωεν βψ τηε τ–ωαλυεσ φορ Θ φρομ τηε 6 παιρσ οφ θ(τ) φρομ ρεπρεσεντατιωε τριαλσ ιν χατσ ανδ ραββιτσ ωιτη αυδιτορψ ανδ ωισυαλ στιμυλι. Τηε ιντερμιττενχψ οφ τηε πεακσ τηρουγηουτ τηε χοντρολ ανδ τεστ περιοδσ ρεσεμβλεσ πρεωιουσ φινδινγσ οφ πηασε χονεσ ρεχυρρινγ ατ ιρρεγυλαρ ιντερωαλσ ιν ανδ βελοω τηε τηετα ρανγε [Φρεεμαν & Βαρριε, 2000; Φρεεμαν, 2003β].

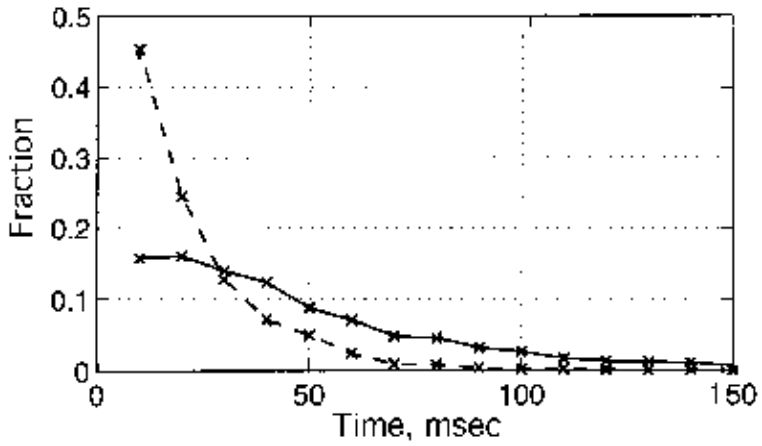

Φιγυρε 7. Ηιστογραμσ αρε σηοων βεφορε σηυφφλινγ (σολιδ χυρωε) ανδ αφτερ (δασηεδ χυρωε) οφ δυρατιονσ ιν μσ οφ εποχησ οφ γλοβαλ σψνχηρονιζατιον ασ μεασυρεδ βψ $\tau_\Theta(\tau)$ ιν Φιγυρε 6. Τηε εποχησ ωιτη λονγ δυρατιονσ αρε ρεμοωεδ βψ σηυφφλινγ.

Power spectral densities of t_Q calculated from individual trials and then averaged over trials showed maxima in the delta range, which were significantly reduced by shuffling the data beforehand [Fig. 8], indicating that the macroscopic synchronization events had recurrence rates comparable to those of mesoscopic wave packets [Fig. 7 in Freeman and Barrie, 2000; Fig. 5 in Freeman, 2002; Figs. 9 and 10 in Freeman and Rogers, 2002]. The autocorrelation of $t_Q(t)$ and the local spatial ensemble averages of the EEG of the 4 cortices and their crosscorrelation were computed to determine the relation of recurrence of peaks in the macroscopic synchronization index, $t_Q(t)$, to activity in the EEG in each area for the cat [Fig. 9, a] and rabbit [Fig. 9, b]. Sharp peaks were found in both species below the theta range, that was found for the cospectra between EEG and phase cones in rabbits [Fig. 3 in Freeman, 2002], and between EEG and global AM patterns in cats [Fig. 7 in Freeman & Burke, 2003]. The high peaks at low frequency in both species conform to the previous findings that the rates of recurrence of significant classification of intracortical AM patterns with respect to discriminated CS [Figs. 9-11 in Freeman, 2003a] were slower than the recurrence rate of intracortical phase cones.

The procedure was repeated using the spatial ensemble average of the simultaneously recorded EEG from all electrodes in all 4 areas [Fig. 10], revealing an apparent species difference in mean repetition rates of peaks in global synchrony.

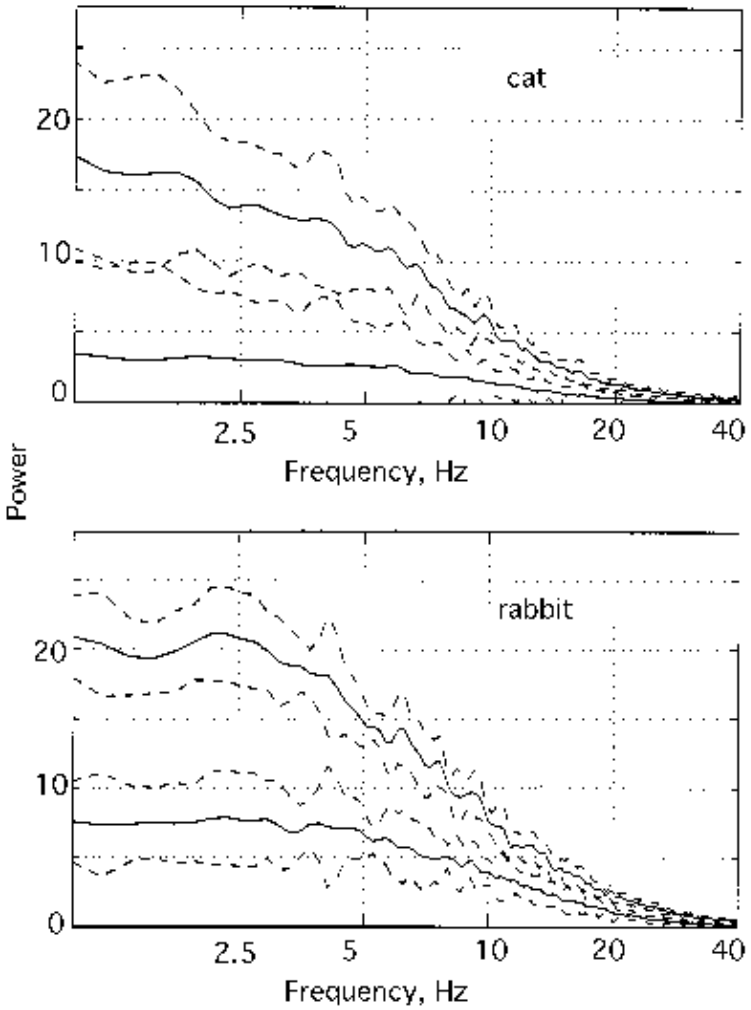

Φιγυρε 8. Ποωερ σπεχτρα ωερε χομπυτεδ φρομ μαχροσχοπιχ σψνχηρονιζατιον ινδεξ, $\tau_{\Theta}(\tau)$, φορ μυλτιπλε τριαλσ ανδ τηεν αωεραγεδ οωερ τριαλσ το γιωε μεανσ (σολιδ χυρωεσ) ανδ στανδαρδ δεωιατιονσ (δασηεδ χυρωεσ). Χομπαρισονσ αρε σηοων φορ χατ ανδ ραββιτ βετωεεν ΕΕΓ δατα (υππερ χυρωεσ) ανδ σηυφφλεδ χοντρολσ (λοωερ χυρωεσ).

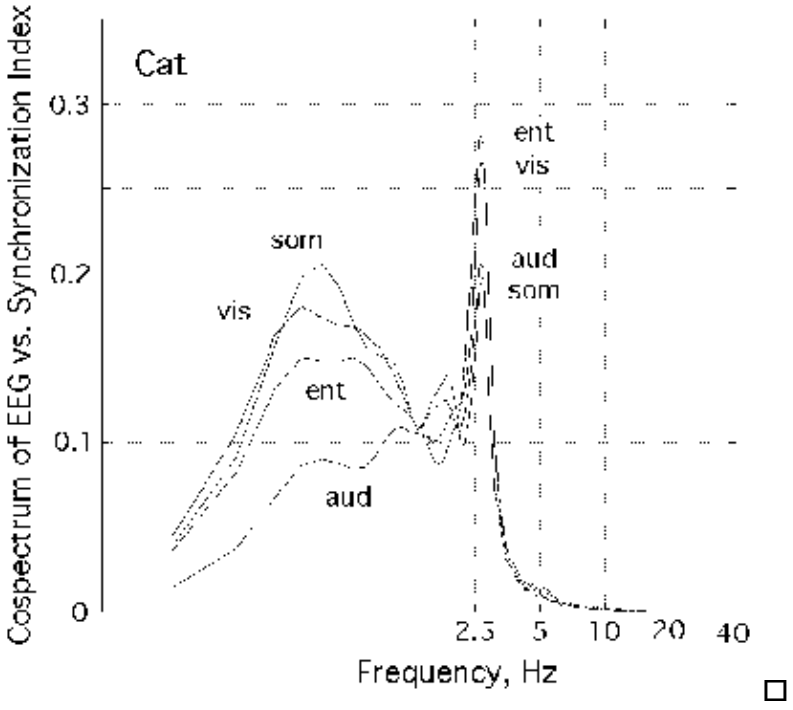

(α)

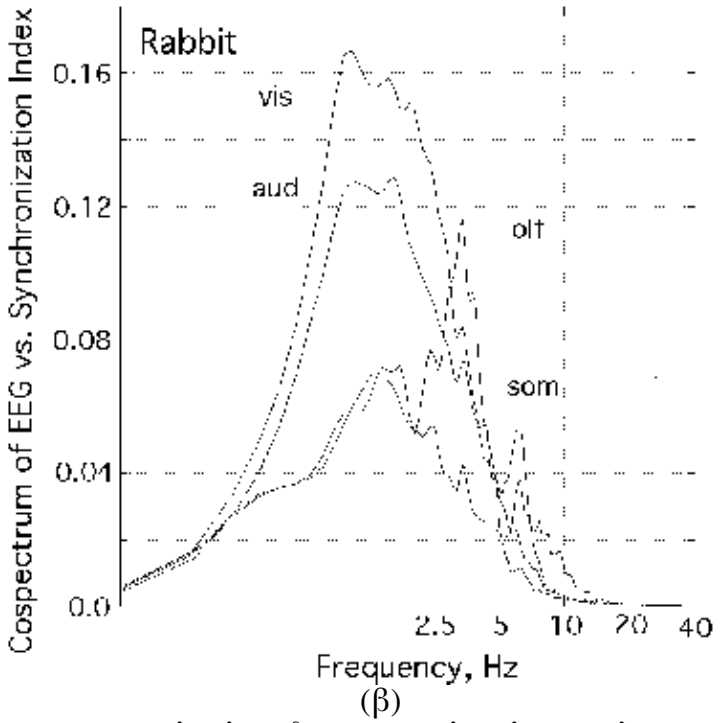

(β)

Φιγυρε 9. Αυτοχορρελατιονσ ωερε χαλχυλατεδ φρομ μυλτιπλε τριαλσ οωερ λοχαλ σπατιαλ ενσεμβλε αωεραγεσ οφ τηε ΕΕΓ οφ εαχη χορτεξ ωιτηουτ φιλτερινγ ανδ φρομ τηε μαχροσχοπιχ σψνχηρονιζατιον ινδεξ, $\tau_{\Theta}(\tau)$ οωερ αλλ χορτιχεσ. Τηε χροσσχορρελατιον ωασ χομπυτεδ βετωεεν εαχη ΕΕΓ ανδ $\tau_{\Theta}(\tau)$, ανδ τηε ΦΦΤ ωασ αππλιεδ το δεριωε τηε φουρ χοσπεχτρα σηοων φορ α χατ (α) ανδ α ραββιτ (β) ιν σεμι−λογ χοορδινατεσ.

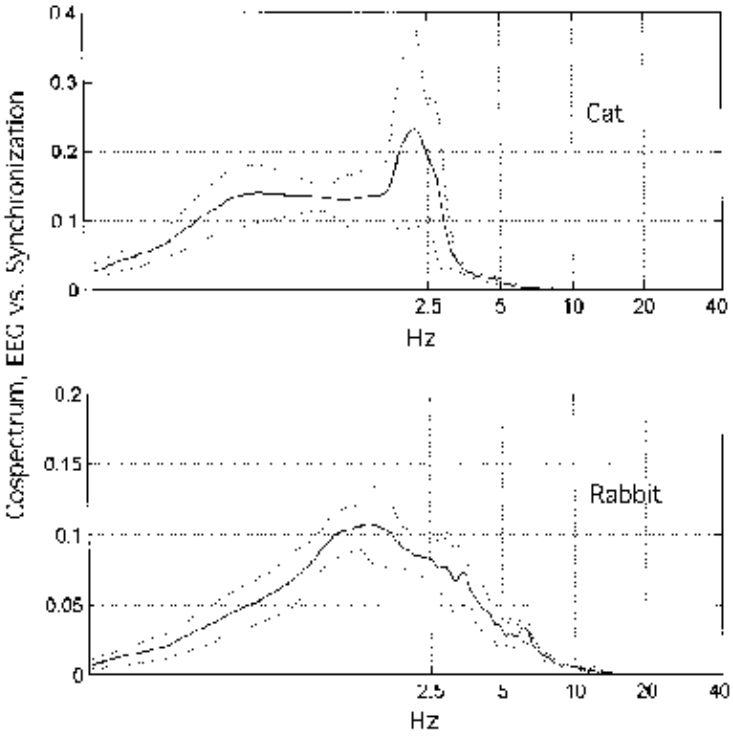

Φιγυρε 10. Τηε χροσσχορρελατιον ωασ χομπυτεδ βετωεεν $\tau_\Theta(\tau)$ ανδ τηε σπατιαλ ενσεμβλε αωεραγε οφ ΕΕΓ σιμυλτανεουσλψ φρομ αλλ αρεασ. Τηε χοσπεχτρα ωερε δεριωεδ βψ τηε ΦΦΤ ανδ αωεραγεδ οωερ αλλ συβφεχτσ το δεριωε μεανσ (σολιδ χυρωεσ) ανδ στανδαρδ δεωιατιονσ αχροσσ συβφεχτσ (δοττεδ χυρωεσ). Τηε σπεχιεσ διφφερενχε βετωεεν πρεδατορ ανδ πρεψ ραισεσ τηε θυεστιον οφ ωηατ μιγητ βε τηε πεακ φρεθυενχψ ιν ηυμανσ.

3.2. Human scalp EEG

The techniques developed in animal research with intracranial electrodes were extended to analysis of the scalp EEG with extracranial electrode arrays. Subjects were asked to control and report their cognitive states and contents during the recording of EEGs prior to extracting AM and PM patterns off-line, in order to measure and correlate the two aspects of cerebral function. Preliminary work in that direction was enabled by a 10-fold advance over prior art in spatial resolution by use of a curvilinear array of 64 electrodes at 3 mm intervals extending 18.9 cm across the scalp [Freeman, Burke, Holmes & Vanhatalo, 2003]. A 10-fold increase in temporal resolution of phase to 5 ms, compared with 50-100 ms with the FFT, was provided by the Hilbert transform giving the analytic phase. In these exploratory studies human subjects were asked to remain at rest with eyes closed, relax their faces and jaws, and then to induce a moderate level of electromyographic potentials (EMG) by tensing their scalp muscles [Fig. 11]. Each of the 64 EEGs was band pass filtered to extract the activity in the beta or gamma range. The Hilbert transform was applied to each signal to calculate the analytic amplitude and phase. The successive time differences in analytic phase were calculated on each channel to approximate the time derivative.

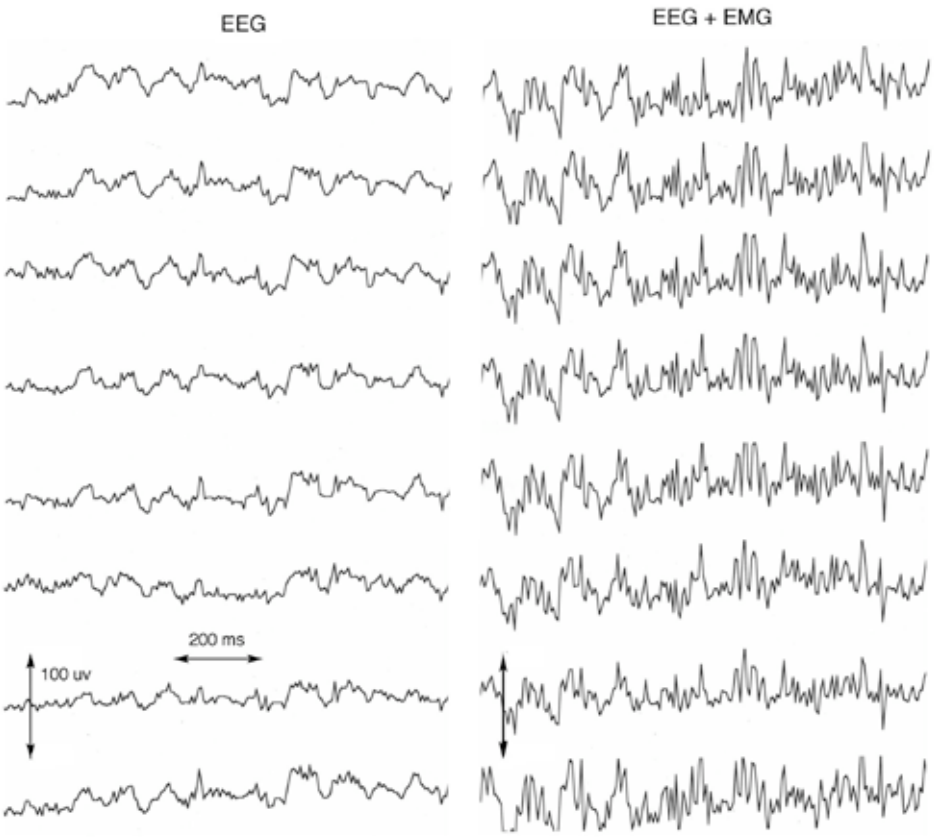

Φιγ. 11. Α σαμπλε οφ 8 χονσεχυτιωε σιγναλσ ισ σηοων φρομ α χυρωιλινεαρ αρραψ οφ 64 ελεχτροδεσ 3 μμ απαρτ εξτενδεδ 18.9 χμ αχροσσ τηε μιδλινε οφ τηε φορεηεαδ οφ α ηυμαν συβφεχτ ατ ρεστ ωιτη εψεσ χλοσεδ (λεφτ) ωηιλε τενσινγ τηε σχαλπ μυσχλεσ το μαινταιν ελεχτρομψογραπηιχ (ΕΜΓ) οσχιλλατιονσ (ριγητ).

An example is shown in Fig. 12 of the 64 channels of sequential phase differences from a subject at rest. The absolute phase differences were plotted in order to facilitate visualization of the PM patterns. The phase differences tended to remain small for epochs of 100-200 ms and then jump briefly to lower or higher values. The jumps tended to occur concomitantly over large distances, sometimes covering the entire array, which in this example was located on the forehead at the hair line across the midline. Calculation of the temporal power spectral density of the cross-correlation between the unfiltered EEG and the signed analytic phase revealed a peak in the alpha range (7-12 Hz), which was not seen in the animals. When the subjects were asked to open their eyes, an intentional act, the coordinated jumps in phase persisted, but the recurrence rate often shifted into the theta range (3-7 Hz) [Freeman, Burke & Holmes, 2003], still higher than the rates found in cats and rabbits [Figs. 8-10].

Determination of the optimal pass band was undertaken by calculating tuning curves. The first step was cross-correlating the unfiltered EEG with the signed phase differences on each channel, calculating the cospectrum, finding the frequency in the alpha or theta ranges at which the power was maximal, and plotting the correlation value for that frequency. Two tuning curves were calculated. First, the high pass filter of the phase differences was fixed at 12 Hz, and the low

pass filter was raised from 20 to 80 Hz in steps of 10 Hz [Fig. 13]. Second, the low pass filter was set at the optimal frequency, and the high pass filter was raised from 4 to 28 Hz in steps of 4 Hz. For most of the 9 subjects and conditions the optimal pass band was 12-30 Hz [Freeman, Burke & Holmes, 2003], as shown in Fig. 12.

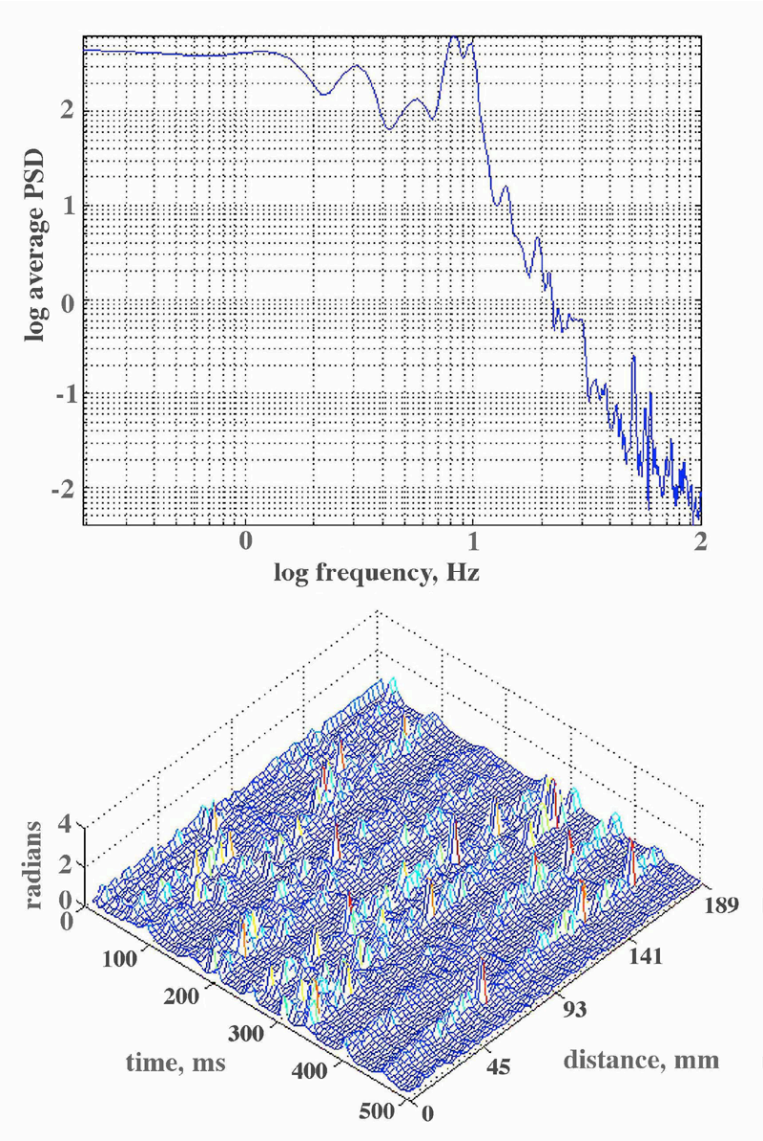

Fig. 12. Upper frame. The cospectrum from the cross-correlation of the unfiltered 64 EEGs with the analytic phase showed the $1/f^{\alpha}$ form with a peak at 10 Hz in the alpha range. **Lower frame:** The 64 EEGs were sampled at 200 Hz and band pass filtered in the beta range (12-30 Hz) before calculation of the analytic phase by the Hilbert transform. The absolute phase differences (ordinate) were plotted as a function of time (left abscissa) for the 64 traces in order (right abscissa) [Freeman, Burke & Holmes, 2003]. The alignment of the concomitant phase jumps parallel to the spatial axis was independent of the orientation of the array on the scalp.

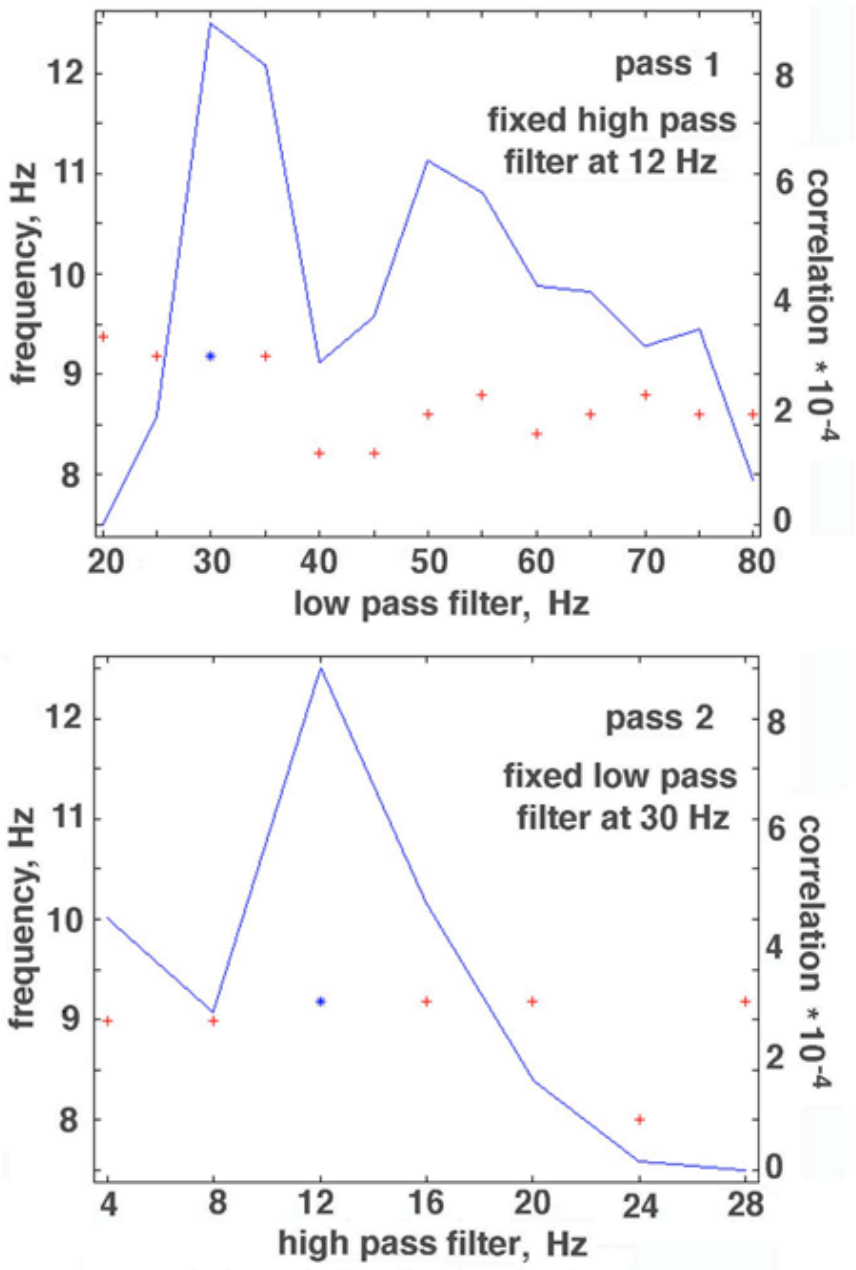

Φιγ. 13. Τηε προχεδυρε ισ ιλλυστρατεδ φορ οπτιμιζινγ τηε πασσ βανδ πριορ το αππλιχατιον οφ τηε Ηιλβερτ τρανσφορμ ιν ρεσπεχτ το δισπλαψ οφ τηε χορρελατιον οφ φυμπσ ιν αναλψτιχ πηασε ωιτη τηε αλπηα ανδ τηετα φρεθυενχψ χομπονεντσ ιν τηε υνφιλτερεδ ΕΕΓ [Φρεεμαν ετ αλ., 2003].

The temporal EEG spectra changed with the intentional action by the subjects of maintaining a modest degree of isometric tension in scalp muscles without movement and with eyes closed [Fig. 14]. The $1/f^{\alpha}$ form resembling that of brown noise [**A**] was replaced with a flat spectrum like that of white noise [**B**]. The alpha peak usually vanished, especially when the eyes were opened, but in this case the alpha peak enlarged and shifted slightly to a higher frequency. The

spatial coordination of the timing of the jumps in the sequential phase differences persisted in both conditions, with some dissociation between the two frontal areas across the midline [**C** and **D**]. Another example is shown in Fig. 15, this from the right hemisphere on a curve 4 cm from the midline and parallel to it. Frame **A** shows the spectrum of the autocorrelation of the 64 unfiltered EEG + EMG during maintenance of muscle tension. Frame **B** shows the cospectrum of the cross-correlation of the unfiltered signals with the signed analytic phase differences after band pass filtering (12-30 Hz). Frame **C** shows the absolute sequential phase differences across the array from anterior (over the frontal lobe) to posterior (over the parietal lobe, with the central sulcus between them. Spatial coordination of phase jumps was typically regional, with occasional instances of alignment across the entire array. For clarification of the apparent discontinuities, advantage was taken of an empirical observation that the analytic amplitude tended to fall to a low value, whenever the analytic phase jumped. The union of these two time series was displayed by converting the analytic amplitude, $A_n(t)$, at time t_n to a weighting function,

$$W_n(t) = 10 \exp[-A_n(t) / 10], \quad (8)$$

and weighting the accompanying phase difference,

$$\Delta\phi_n(t) = W_n(t) [\phi(t_n) - \phi(t_{n-1})]. \quad (9)$$

The values of W ranged from near zero for high A to 1 for zero A. Display of this union is shown in frame **D** for the same data as in frame **C**.

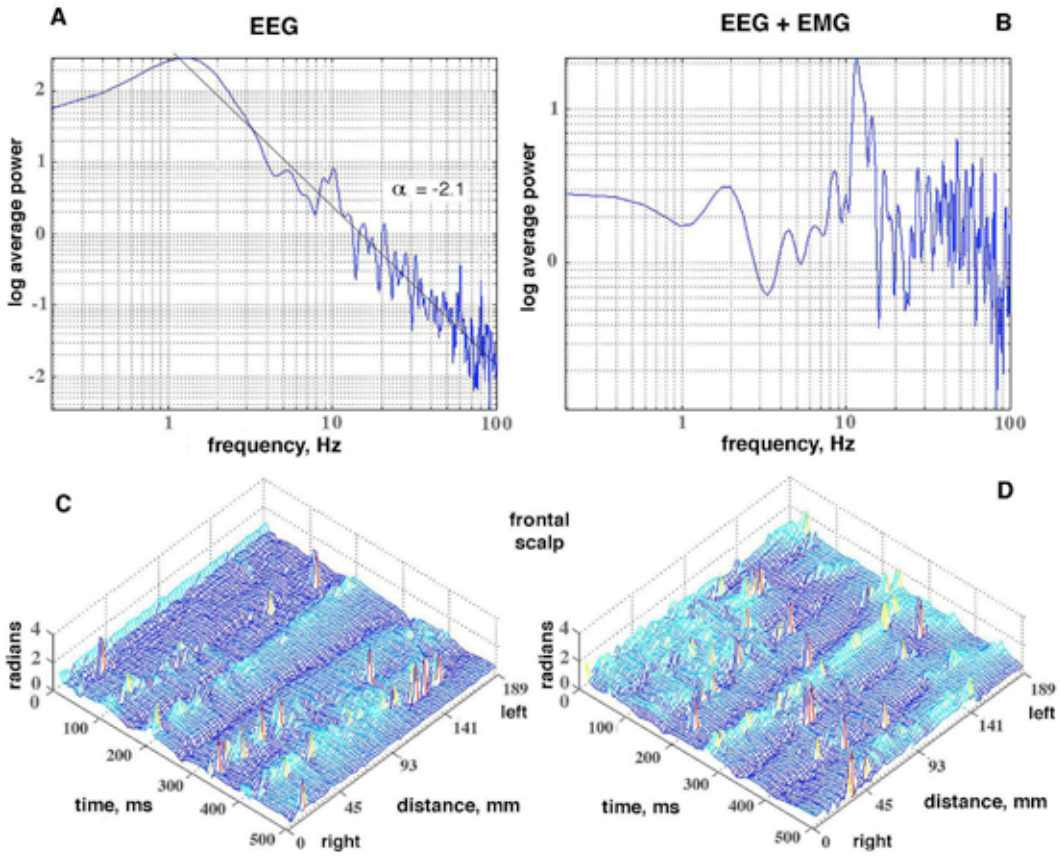

Φιγ. 14. Αν εξαμπλε ισ σηοων οφ τηε χηανγεσ ιν ποωερ σπεχτραλ δενσιτψ οφ τηε ΕΕΓ ωιτη τηε ονσετ οφ ιντεντιοναλ ΕΜΓ. Τηε χηανγεσ ινχλυδε τηε αδδιτιον οφ σχαλπ μυσχλε ποτεντιαλσ ανδ τηε χηανγε ιν βραιν στατε ωιτη ινδυχτιον οφ αν ιντεντιοναλ αχτιον.

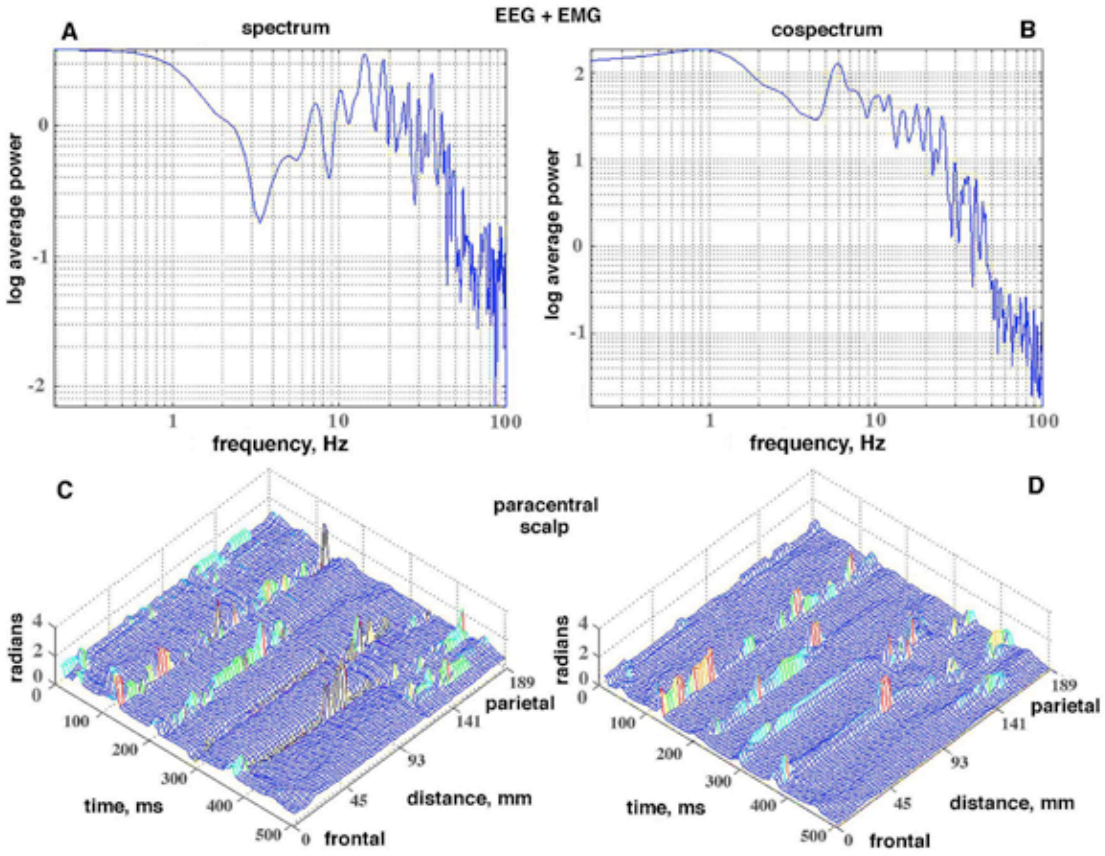

Φιγ1ξ5ΑΒΤηεσπεχτρυμοφτηεαυτοχορρελατιογοφτηεΕΕΓΕΜΓισχομπαρεδωιτητηεχοσπεχτρυμοφ τηεχροσσχορρελατιογοφτηευνφιλτερεδσιγναλσωιτητηεσιγνεδαναλψτιχπηασεδιφφερενχεσογ τηε64χηαννελσΧΤηεσπατιαλσψνχηρονψοφτηεαβσολυτεωαλυεσοφτηεπηασεφυμπσωασφουν δτοχοωερλονγδιστανχεσωιτηδισσοχιατιογαππαρεντβετωεεγτηεφρονταλανδπαριεταλρεγιονσ οφτηεαρραψΤηεβρεακποιντμαψηαωεχορρεσπονδεδτοτηελοχατιογοφτηεχεντραλσυλχυσ;χον φιρματιογωουλδηαωερεθυιρεδΜΡΙΔΤηεπηασεδιφφερενχεσωερεωειγητεδβψτηεαναλψτιχαμ πλιτυδεσηοωινγτηευνιογοφτηεπηασεφυμπσανδμινιμαιντηεαναλψτιχαμπλιτυδε[εθυατιονσ8αν δ9]

4. DISCUSSION

4.1. Comparison of local and global phase patterns

The novel observations on phase in this report depended on five technical innovations. First, multiple small high density electrode arrays were placed on several strategic areas of the same hemisphere [Gaál & Freeman, 1998; Freeman, Gaál & Jornten, 2003]. Second, the standard error of phase measurement was minimized by optimization of spatial and temporal filters [Freeman and Viana Di Prisco, 1986]. Third, the ranges of gamma activity, which differed between species [Bressler and Freeman, 1980], were delineated for rabbits and cats by optimizing the classification of AM patterns in EEG of sensory receiving areas with respect to behavior [Freeman and Baird, 1987; Barrie, Lenhart and Freeman, 1996; Freeman & Barrie, 2003]. Fourth, the criterion for phase synchronization was broadened to include stabilized nonzero spatial phase distributions over brief time periods, in which phase gradients could be identified in the gamma range of neocortical EEGs of sensory receiving areas. Fifth, the Hilbert transform provided greater temporal resolution than was possible with Fourier and wavelet techniques of phase measurement and gave evidence for 1st order state transitions by which AM patterns formed [Freeman and Rogers, 2002].

Prior studies addressing individual sensory cortices revealed local patterns of phase modulation (PM) at frequencies in the gamma range. In the spatial domain the gradients in radians/mm, when expressed in m/s using the frequency, corresponded to the conduction velocities of the axons running parallel to the surface. The PM patterns lasted 80-100 ms and recurred at rates in the theta range (3-7 Hz) [Freeman Baird, 1987; Freeman & Barrie, 2000]. In the time domain the local synchronization index, q(t), showed sustained high levels punctuated by brief episodes of decoherence. This temporal organization included brief episodes of increase in the spatial standard deviation, SD_x [Freeman & Rogers, 2003]. The peaks in the SD were associated with spikes in the temporal derivative of the analytic phase on multiple channels. The spikes coincided within the 4-8 ms time window predicted from the phase velocity and the width of the electrode array. The present study revealed similar properties that differed in important respects. A sustained relatively low level of synchrony among multiple cortices as measured by $t_Q(t)$ was punctuated by with brief episodes of increased synchrony. The recurrence rates of the peaks were in the delta range (1-3 Hz). The reciprocals of these low rates corresponded to the time intervals between AM patterns that were classified at better than chance levels with respect to discriminative CSs, both for individual sensory cortices [Fig. 12 in Barrie, Freeman & Lenhart, 1996], particularly with use of phase gradients to locate AM patterns by Fourier decomposition [Fig. 8 in Freeman & Barrie, 2000] and by wavelet decomposition [Figs. 12-14 in Freeman, 2003b]. The intervals between the peaks of correct classification of multisensory AM patterns from RMS measurements [Figs. 5-7 in Freeman & Burke, 2003] likewise lay in the delta range.

The low recurrence rates and longer intervals of peaks in $t_Q(t)$ were consistent with the way in which the measure was defined: a low variance around a high mean gave a high peak value. The global pattern implied that local wave packets maintained relatively long duty cycles, with brief breaks into decoherence and reorganization at times that were internally determined, and that $t_Q(t)$ captured the moments when all areas were locally synchronized and thereby transmitting strongly at the same time. The union was expressed in a global AM pattern, not in a "burst" of

high amplitude. This expression also characterized local AM patterns, particularly in the olfactory bulb where mean amplitude typically fell with CS onset [Kay & Freeman, 1998] and AM pattern emergence. In optimizing the classification of AM patterns with respect to CSs, an important step is to discard the information about global amplitude by normalizing each AM pattern vector to zero mean and unit standard deviation. While an increase in global amplitude could manifest a decrease in phase dispersion, an amplitude decrease could express an increase in constraints among bulbar neurons due to enhanced synaptic interactions during systolic transmission. This interpretation is consistent with numerous reports of enhanced gamma activity in various brain regions, as shown by scalp EEGs of humans engaged in a variety of cognitive tasks [e.g., Müller et al., 1996; Tallon-Baudry et al., 1996, 1998; Miltner et al., 1999; Rodriguez et al., 1999; Müller, 2000; Csibra et al., 2000]. This is because a spatial pattern must have both high and low amplitudes at locations that are consistent across trials, and the high amplitude sites tend to stand out more clearly from the variance than do the low amplitude sites, while the mean is uninformative.

4.2. Spectral scaling and self-organized criticality

A striking feature of the putative macroscopic phase jumps is the narrow time window in which they are coordinated across astonishing cortical distances. This temporal confinement is not apparent with the global synchronization index, owing to coarse-graining of the animal data with the 80 ms window, whereas it is readily seen in the human EEG data with the numerical derivative of the analytic phase, up to the limit of the digitizing interval (5 ms). The onset of an AM pattern appears to involve a discontinuity in cortical function in the nature of a first order phase transition resembling a subcritical Hopf bifurcation. The question is how the long-range global state changes come about virtually simultaneously, despite the constraint of the finite axon conduction velocity.

Part of an answer has already been alluded to [Freeman, 2003a] in the concept of self-organized criticality (SOC) [Bak, Tang and Wiesenfeld, 1987]. According to this hypothesis a large system can hold itself in a near-unstable state, so that by a multitude of adjustments it can adapt to environments that change continually and unpredictably. While most of the adaptive adjustments last only a few ms, some may last long enough to manifest salient steps by which brains adapt to important features of the environment, such as the arrival of an expected CS. Studies of SOC indicate that the few long-lasting epochs at unusual intervals can be expected to have large spatial extents as well, but short durations and sizes predominate numerically.

In the histogram of time durations between jumps in analytic phase the number increased exponentially with decreasing duration to the limit set by the digitizing step [Fig. 7]. A lower limit on duration was defined for phase cones by maximizing the cospectral peak in the theta range, which was derived from the FFT after cross-correlating the time series of cone formation with the on-going EEG [Freeman, 2002], but without this restriction there was no lower limit other than the digitizing interval. A lower limit on the duration of AM patterns was assigned by optimizing the classification rate with respect to classes of CS [Barrie, Freeman and Lenhart, 1996]. Only as a result of using this constraint were the recurrence rates of AM patterns in the theta and delta ranges. Without the criteria of correlation with EEGs and CSs, the distributions of AM and PM pattern size and duration appeared to be fractal. This interpretation is consistent

with the $1/f^{\alpha}$ form of scaling in both the temporal and spatial spectra [Freeman & Baird, 1987; Freeman & van Dijk, 1987; Barrie, Lenhart & Freeman, 1996; Freeman, Burke, Holmes & Vanhatalo, 2003], which as shown in Fig. 12 differs markedly from the relatively flat spectra of the EMG.

The picture that emerges shows the cortex as a seething and volatile continuum that robustly maintains itself at the edge of a stable state, from which emerge transient coordination of neural firings, most of which lapse and disappear, but some of which coalesce and grow instantly, owing to priming from the limbic system and to the impact of sensory input from the environment. This may clarify the tripartite distinction used in this tutorial. Microscopic refers to neurons; macroscopic refers to behavior; and mesoscopic refers to the intervening realm of neural populations. The AM and PM patterns bridge the three levels.

A further insight is required from advanced physics to interpret these EEG data. As already noted [Freeman, 1999] there is a disparity between the time limit imposed on the transfer of information in brains by the conduction velocity of action potentials on axons and the appearance of zero lag among events at large distances, at least to the grain of measurement. This is analogous to the phenomenon of anomalous dispersion in media conducting light or sound energy [Hecht & Zajac, 1974, discussed in Freeman, 2003a]. A distinction is required between the group velocity in a neural population, which is the rate at which information can be disseminated by axonal propagation and synaptic integration, versus the phase velocity at which a change in state can spread through the population. Just as in an axon the stored energy that is required for the change in state from rest to an action potential is released by a weak triggering current pulse, so in a population the energy of synaptic interactions is held in readiness for an explosive change from one pattern of organization to another. The holding is a fine balancing act, in which small fluctuations are continually quenched, but the fluctuations manifest the readiness, so that with eventual release a cascade gives a dramatic wave of the kind that sweeps over the scalp as shown in Figs. 12 to 14. SOC cannot tell the whole story, because that does not explain the prominent peaks in the classical ranges of the EEG (delta, theta, alpha, beta and gamma), nor does it include the regulatory roles of the thalamus, brain stem, and limbic system, but SOC helps substantially to explain the cortical mechanism that is being regulated.

4.3. Limitations on identifying the neural correlates of cognition from EEG and behavior

Peaks in the intercortical macroscopic synchronization index, $t_Q(t)$, occurred with equal likelihood before and after CS onsets. This is evidence that cognitive activity in animal brains does not start and end with stimulus and response but extends throughout the intentional cycle of expectancy, sensation, perception, and action. Many and perhaps all parts of the cerebral hemisphere participate in each new state of expectancy at the start of each trial. That brain state can be conceived as a point in brain state space moving discontinuously on a high-dimensional trajectory. Upon the arrival of a CS, the trajectory that the parts created cooperatively diverges abruptly from a domain of expectancy and passes through a sequence of 2-4 states governed by macroscopic attractors, which are largely determined from past experience, and which are selected by the convergence of wave packets, culminating in each trial in a CR. Within 300-500 ms after CS onset, every cortex is up-dated by what has happened in every other cortex [Ohl, Scheich and Freeman, 2001]. For example, a neural activity pattern in the visual area in

response to a sighting of prey should retain its modality specificity, while changing in respect to the odor or sound of prey, and to the evolving spatial relation of self in pursuit of prey.

The weakest link in this proposed chain of evidence for nonlocal cortical function is a test (not yet fully successful) to determine whether the episodes of phase decoherence can serve to identify the locations of AM patterns that can be classified optimally with respect to CSs. Prior efforts to answer this question were only partially successful, because the starting and ending times of AM and PM patterns were not clearly demarcated. They varied unpredictably from each trial to the next. The patterns were statistically related to CSs and to EEG components in the delta, theta and alpha ranges, but the averages did not carry over well into single trial analysis. These experimental difficulties were compounded by the lack of objective criteria by which to define classes of macroscopic states. For primary receiving cortices mediating sensation into wave packets at the mesoscopic level, the CSs and CRs provided acceptable criteria. For subsequent operations involving perception, the correlates of EEG patterns are states of meaning, and the classes may deviate from both CSs and CRs in unknown ways. There is no way to tell what animals are thinking, only what they are intending, and that solely from their histories and actions. For this reason the further development of a theory of meaning based in brain dynamics will require studies of brain activity in normal volunteers. That is why the rapid deployment of EEG analysis to scalp recordings is so important. Humans have formidable talents for expressing what they mean as well as intend, and the close cooperation of subjects with biologists, psychologists, and engineers will be essential.

ACKNOWLEDGMENTS

This work was funded by research grants from NIMH (MH06686), ONR (N63373 N00014-93-1-0938), NASA (NCC 2-1244), and NSF (EIA-0130352). The authors are grateful to John M. Barrie, Gyöngyi Gaál, Brian Lau and Maritza Alvarado for assistance in collection of the data from rabbits and cats, and to Brian Burke and Robert Kozma for assistance in programming and software development.

REFERENCES

Barrie, J. M., Freeman, W. J. & Lenhart, M. [1996] Modulation by discriminative training of spatial patterns of gamma EEG amplitude and phase in neocortex of rabbits. *J. Neurophysiol.* **76**: 520-539.

Βασαρ, Ε. [1998] *Βραιν Φυνχτιον ανδ Οσχιλλατιονσ.* (Σπρινγερ–ζερλαγ, Βερλιν).

Βρεσσλερ, Σ. Λ. [1996] Ιντεραρεαλ σψνχηρονιζατιον ιν τηε ϖισυαλ χορτεξ. *Βεηατϖ. Βραιν Ρεσ.* **76**: 37–49

Βρεσσλερ, Σ. Λ., Χοππολα, Ρ. & Νακαμυρα, Ρ. [1993] Επισοδιχ μυλτιρεγιοναλ χορτιχαλ χοηερενχε ατ μυλτιπλε φρεθυενχιεσ δυρινγ ϖισυαλ τασκ περφορμανχε. *Νατυρε* **366**: 153–156.

Βρεσσλερ, Σ. Λ. & Φρεεμαν, Ω. ϑ. [1980] Φρεθυενχψ αναλψσισ οφ ολφαχτορψ σψστεμ ΕΕΓ ιν χατ, ραββιτ ανδ ρατ. *Ελεχτροενχεπη. χλιν. Νευροπηψσιολ.* **50**: 19–24.

Csibra, G., Davis, G., Spratling, M. W. & Johnson, M. H. [2000] Gamma oscillations and object processing in the infant brain. *Science* **290**: 1582-1585.

Δυμενκο, ς. Ν. [1970] Ελεχτροενχεπηαλογραπηιχ ινϖεστιγατιον οφ χορτιχαλ ρελατιονσηιπσ ιν δογσ δυρινγ φορματιον οφ α χονδιτιονεδ ρεφλεξ στερεοτψπε. Ιν: Ρυσινοϖ, ς. Σ. (εδ.) *Ελεχτροπηψσιολογψ οφ τηε Χεντραλ Νερϖουσ Σψστεμ*, Ηαιγη, Β. (τρανσ.), Δοτψ, Ρ. Ω. (εδ.). (Πλενυμ Πρεσσ, Νεω Ψορκ), ππ. 107–118.

Δυμενκο, ς. Ν. [2000] Τηε φυνχτιοναλ σιγνιφιχανχε οφ ηιγη–φρεθυενχψ χομπονεντσ οφ βραιν ελεχτριχαλ αχτιϖιτψ. Ιν: *Χομπλεξ Βραιν Φυνχτιονσ: Χονχεπτυαλ Αδϖανχεσ ιν Ρυσσιαν Νευροσχιενχε.* Μιλλερ, Ρ., Ιϖανιτζκψ, Ι & Βαλαβαν, Π. (εδσ.). (Ηαρωοοδ Αχαδεμιχ Πυβλ., Αμστερδαμ ΝΛ), ππ. 129–150.

Engel, A. K., Fries, P., König, P., Brecht, M. & Singer, W. [1999] Temporal binding, binocular rivalry, and consciousness. *Consciousness & Cognition* **8**: 128-151.

Freeman, W.J. [1975] *Mass Action in the Nervous System.* (Academic Press, New York).

Freeman, W.J. [1979] EEG analysis gives model of neuronal template-matching mechanism for sensory search with olfactory bulb. *Biol. Cybern.* **35**: 221-234.

Freeman, W.J. [1980] Use of spatial deconvolution to compensate for distortion of EEG by volume conduction. *IEEE Trans. Biomed. Engin.* **27**: 421-429.

Freeman, W.J. [1983] The physiology of mental images. *Biol. Psychiat.* **18**: 1107-1125.

Freeman, W.J. [1991] The physiology of perception. *Sci. Amer.* **264**: 78-85.

Freeman, W.J. [2000] *Neurodynamics. An Exploration of Mesoscopic Brain Dynamics.* (Springer-Verlag, London UK).

Freeman, W.J. [2003a] A neurobiological theory of meaning in perception. Part 1. Information and meaning in nonconvergent and nonlocal brain dynamics. *Int. J. Bifurc. Chaos* 13: 2493-2511.

Freeman, W.J. [2003b] A neurobiological theory of meaning in perception. Part 2. Spatial patterns of phase in gamma EEG from primary sensory cortices reveal the properties of mesoscopic wave packets. *Int. J. Bifurc. Chaos* 13: 2513-2535.

Freeman, W.J. & Baird, B. [1987] Relation of olfactory EEG to behavior: Spatial analysis: *Behav. Neurosci.* **101**: 393-408.

Φρεεμαν, Ω.θ. & Βαρριε, θ. Μ. [2000] Αναλψσισ οφ σπατιαλ παττερνσ οφ πηασε ιν νεοχορτιχαλ γαμμα ΕΕΓσ ιν ραββιτ. θ. *Νευροπηψσιολ.* **84**: 1266–1278.

Freeman, W.J. & Burke, B.C. [2003d] A neurobiological theory of meaning in perception. Part 4. Multicortical patterns of amplitude modulation in gamma EEG. *Int. J. Bifurc. Chaos* 13: 2857-2866.

Freeman, W.J., Burke, B.C. & Holmes, M.D. [2003] Aperiodic phase re-setting in scalp EEG of beta-gamma oscillations by state transitions at alpha-theta rates. Human Brain Mapping 19: 248-272.

Freeman, W.J., Burke, B.C., Holmes, M.D. & Vanhatalo, S. [2003] Spatial spectra of scalp EEG and EMG from awake humans. Clin. Neurophysiol. 114: 1050-1060.

Freeman, W.J. & Davis, G.W. [1990] Olfactory EEG changes under serial discrimination of odorants by rabbits. pp. 375-391 in: Schild D (ed.) *Chemosensory Information Processing, NATO ASI Series, Vol. H39*. (Springer-Verlag, Berlin).

Φρεεμαν, Ω.θ., Γα□λ, Γ. & θορντεν, Ρ. [2003] Α νευροβιολογιχαλ τηεορψ οφ μεανινγ ιν περχεπτιον. Παρτ 3. Μυλτιπλε χορτιχαλ αρεασ σψνχηρονιζε ωιτηουτ λοσσ οφ λοχαλ αυτονομψ.*Ιντ. θ. Βιφυρχ. Χηαοσ*: ιν πρεσσ.

Φρεεμαν, Ω.θ. & Ρογερσ, Λ. θ. [2002] Φινε τεμποραλ ρεσολυτιον οφ αναλψτιχ πηασε ρεωεαλσ επισοδιχ σψνχηρονιζατιον βψ στατε τρανσιτιονσ ιν γαμμα ΕΕΓσ. θ. *Νευροπηψσιολ.*, **87**, 937–945.

Freeman, W.J. & Rogers, L.J. [2003] A neurobiological theory of meaning in perception. Part 5. Multicortical patterns of phase modulation in gamma EEG. *Int. J. Bifurc. Chaos* : i2867-2887.

Freeman, W.J. & Schneider, W. [1982] Changes in spatial patterns of rabbit olfactory EEG with conditioning to odors. *Psychophysiol.* **19**: 44-56.

Freeman, W.J. & Van Dijk, B. [1987] Spatial patterns of visual cortical fast EEG during conditioned reflex in a rhesus monkey. *Brain Res.* **422**: 267-276.

Freeman, W.J. & Viana Di Prisco, G. [1986] Relation of olfactory EEG to behavior: Time series analysis. *Behav. Neurosci.* **100**: 753-763.

Γα□λ, Γ. & Φρεεμαν, Ω.θ. [1998] Ρελατιονσ αμονγ ΕΕΓσ φρομ εντορηναλ χορτεξ, ολφαχτορψ βυλβ, σοματομοτορ, αυδιτορψ ανδ ωισυαλ χορτιχεσ ιν τραινεδ χατσ. Ιν: Δινγ, Μ., Διττο, Ω., Πεχορα, Λ., Σπανο, Μ. & ζοηρα, Σ., εδσ., *Προχ. 4τη Εξπερ. Χηαοσ Χονφ.* (Ωορλδ Σχιεντιφιχ, Σινγαπορε), πп. 179–184.

Gevins, A.S., Bressler, S. L., Morgan, N., Cutillo, B., White, R., Greer, D. & Illes, J. [1989] Event-related covariances during a bimanual visuomotor task. *Electroenceph. clin. Neurophysiol.* **74**: 58-75.

Ηαιγ, Α.Ρ., Γορδον, Ε., Ωριγητ, θ.θ., Μεαρεσ, Ρ.Α. & Βαηραμαλι, Η. [2000] Σψνχηρονουσ χορτιχαλ γαμμα–βανδ αχτιωιτψ ιν τασκ–ρελεωαντ χογνιτιον. *ΝευροΡεπορτ* **11**: 669–675.

Kaernbach, C., Schroger, E., Jacobsen, T. & Roeber, U. [1999] *NeuroReport* **10**: 713-716.

Λαχηαυξ, θ Π. , Ροδριγυεζ, Ε., Μαρτινεριε, θ. & ζαρελα, Φ.θ. [1999] Μεασυρινγ πηασε σψνχηρονψ ιν βραιν σιγναλσ. *Ηυμαν Βραιν Μαππινγ* **9**:194–208.

Lashley, K.S. [1960] *The Neuropsychology of Lashley; Selected Papers*. Beach, F. A. et al. (eds.). (McGraw-Hill, New York).

Λεημανν, Δ. & Μιχηελ, Χ.Μ. [1990] Ιντραχερεβραλ διπολε σουρχε λοχαλιζατιον φορ ΦΦΤ ποωερ μαπσ. *Ελεχτροενχεπη. χλιν. Νευροπηψσιολ.* **76**: 271–276.

Λυυ, Π., Φλαιση, Τ. & Τυχκερ, Δ.Μ. [2000] Μεδιαλ φρονταλ χορτεξ ιν αχτιον μονιτορινγ. θ. *Νευροσχιενχε* 20: 464–469.

Menon, V., Freeman, W.J., Cutillo, B.A., Desmond, J.E., Ward, M.F., Bressler, S.L, Laxer, K.D., Barbaro, N.M. & Gevins, A.S. [1996] Spatio-temporal correlations in human gamma band electrocorticograms. *Electroenceph. clin. Neurophysiol.* **98**: 89-102.

Müller, M.M., Bosch, J., Elbert, T., Kreiter, A., Valdes Sosa, M., Valdes Sosa, P. & Rockstroh, B. [1996] Visually induced gamma band responses in human EEG - A link to animal studies. *Exper. Brain Res.* **112**: 96-112.

Müller, M.M. [2000] Hochfrequente oszillatorische Aktivitäten im menschlichen Gehirn. *Zeitschrift für Exper. Psychol.* **47**: 231-252.

Miltner, W H.R., Barun, C., Arnold, M., Witte, H, & Taub, E. [1999] Coherence of gamma-band EEG activity as a basis for associative learning. *Nature* **397**: 434-436.

Μινγζηου, Δ., Βρεσσλερ, Σ.Λ., Ψανγ, Ω. & Λιανγ, Η. [2000] Σηορτ–ωινδοω σπεχτραλ αναλψσισ οφ χορτιχαλ εωεντ–ρελατεδ ποτεντιαλσ βψ αδαπτιωε μυλτιωαριατε αυτορεγρεσσιωε μοδελινγ: δατα πρεπροχεσσινγ, μοδελ ωαλιδατιον, ανδ ωαριαβιλιτψ ασσεσσμεντ. *Βιολ. Χψβερν.* **83**: 35–45.

Ngo, T.T.; Miller, S.M., Liu, G.B & Pettigrew, J.D. [2000] Binocular rivalry and perceptual coherence. *Current Biol.* **10**: 134-136.

Νυνεζ, Π.Λ. [1981] *Ελεχτριχ Φιελδσ οφ τηε Βραιν: Τηε Νευροπηψσιχσ οφ ΕΕΓ.* (Οξφορδ Υνιω. Πρεσσ, Νεω Ψορκ).

Νυνεζ, Π.Λ., Σρινιωασαν, Ρ., Ωεστδορπ, Α.Φ., Ωιφεσινγηε, Ρ.Σ., Τυχκερ, Δ.Μ., Σιλβερστειν, Ρ.Β. & Χαδυσχη, Π.θ. [1997] ΕΕΓ χοηερενχψ Ι: στατιστιχσ, ρεφερενχε ελεχτροδε, ωολυμε χονδυχτιον, Λαπλαχιανσ, χορτιχαλ ιμαγινγ ανδ ιντερπρετατιον ατ μυλτιπλε σχαλεσ. *Ελεχτροενχεπηρ. χλιν. Νευροπηψσιολ.* **103**: 499–515.

Ohl, F.W., Scheich, H. & Freeman, W.J. [2001] Change in pattern of ongoing cortical activity with auditory category learning. *Nature* **412**: 733-736.

Pavlov, I.P. [1960] *Conditioned Reflexes; An Investigation of the Physiological Activity of the Cerebral Cortex.* Anrep, G. V. (trans., ed.). (Dover Publ., New York).

Pikovsky, A., Rosenblum, M. & Kurths, J. [2001] .*Synchronization: A Universal Concept in Nonlinear Sciences.* (Cambridge U.P., Cambridge UK).

Pribram, K.H. [1971] *Languages of the Brain; Experimental Paradoxes and Principles in Neuropsychology.* 9Prentice-Hall, Englewood Cliffs, N.J.).

Quiroga, R.Q., Kraskov, A., Kreuz, T. & Grassberger, P. [2002] Performance of different synchronization measures in real data: A case study on electroencephalographic signals. *Physical Rev. E* **6504**:U645-U658 - art. no. 041903.

Rodriguez, E., George, N., Lachaux, J.-P., Martinerie, J., Renault, B. & Varela, F.J. [1999] Perception's shadow: long-distance synchronization of human brain activity. *Nature* **397**: 430-433.

Σηεερ, Δ. [1976] Φοχυσεδ αρουσαλ ιν 40–Ηζ ΕΕΓ. Ιν: Κνιγητ, Ρ. Μ. & Βακκερ, Δ. θ. (εδσ.) *Τηε Νευροπσψχηολογψ οφ Λεαρνινγ Δισορδερσ.*)(Υνιω. Παρκ Πρεσσ, Βαλτιμορε ΜΔ), ππ. 71–87.

Sheer, D. E. [1989] Sensory and cognitive 40-Hz event-related potentials: Behavioral correlates, brain function, and clinical application. In: *Brain Dynamics.* Basar, E. & Bullock, T. H. (eds.), (Springer-Verlag, Berlin).

Σρινιωασαν, Ρ., Νυνεζ, Π. Λ. & Σιλβερστειν, Ρ. Β. [1998] Σπατιαλ φιλτερινγ ανδ νεοχορτιχαλ δψναμιχσ: εστιματεσ οφ ΕΕΓ χοηερενχε. *IEEE Τρανσ. Βιομεδ Ενγιν.* **45**: 814–826.

Tallon-Baudry, C., Bertrand, O., Delpuech, C. & Pernier, J. [1996] Stimulus-specificity of phase-locked and non phase-locked 40-Hz visual responses in human. *J. Neurosci.* **16**: 4240-4249.

Tallon-Baudry, C., Bertrand, O., Peronnet , F. & Pernier J. [1998] Induced gamma-band activity during the delay of a visual short-term memory task in humans. *J. Neurosci.* **18**: 4244-4254.

Τασσ, Π., Κυρτησ, θ., Ροσενβλυμ, Μ., Ωευλε, θ., Πικοωσκψ, Α., ζολκμανν, θ., Σχηνιτζλερ, Η. & Φρευνδ, Η. [1999] Χομπλεξ πηασε σψνχηρονιζατιον ιν νευροπηψσιολογιχαλ δατα. Ιν: *Αναλψσισ οφ Νευροπηψσιολογιχαλ Βραιν Φυνχτιονινγ*. Υηλ, Χ. (εδ.), (Σπρινγερ–ζερλαγ, Βερλιν), ππ. 252–273.

ωον Στειν, Α., Ραππελσβεργερ, Π., Σαρντηειν, θ. & Πετσχηε, Η. [1999] Σψνχηρονιζατιον βετωεεν τεμποραλ ανδ παριεταλ χορτεξ δυρινγ μυλτιμοδαλ οβφεχτ προχεσσινγ ιν μαν. *Χερεβραλ Χορτεξ* **9**:137–150.

Young, R. M. [1970] *Mind, Brain and Adaptation in the Nineteenth Century: Cerebral Localization and its Biological Context from Gall to Ferrier*. (Clarendon Press, Oxford UK).